Development of Prediction Models on Base-Catalyzed Hydrolysis Kinetics of Phthalate Esters with Density Functional Theory Calculation

Tong Xu, Jingwen Chen,* Zhongyu Wang, Weihao Tang, Deming Xia, Zhiqiang Fu, Hongbin Xie

Key Laboratory of Industrial Ecology and Environmental Engineering (Ministry of Education), School of Environmental Science and Technology, Dalian University of Technology, Dalian 116024, China

*Corresponding author phone/fax: +86-411-84706269; e-mail: jwchen@dlut.edu.cn

Contents

Global minimum search. The search for global minimum of various conformations was carried out by TURBOMOLE program.[1] *Ab initio* molecular dynamics (AIMD) was used to generate possible conformations at the B-LYP/Def2-SV(P) level, with resolution-of-the-identity (RI) used to accelerate the computation.[2] During the generation of conformations, temperature (*T*) was set as 500 K and simulation steps were set as 5000. Other parameters for AIMD were adopted as reported by Li et al.[3] Among 5000 conformations generated from AIMD, about 30 representative conformations were selected for further optimization and calculation of the single point energy. The conformation with the lowest energy was chosen for further calculations.

Energy calculation. Gibbs free energies (*G*) for all structures were calculated by combining the single point energies at the B3LYP/6-311++G(3df,2pd) level and Gibbs free energy correction terms at the B3LYP/6-311++G(2d,2p) level. Energies (*E*) for carboxylic acid esters were calculated by combining the single point energies at the B3LYP/6-311++G(3df,2pd) level and zero point energy correction terms at the B3LYP/6-311++G(2d,2p) level. Activation energy (E_a) values were calculated by the difference between *E* of reactants and *E* of transition states of rate-determining steps. *G* relates enthalpy (*H*) and entropy (*S*) contributions by $\Delta G = \Delta H - T\Delta S$, and *H* relates *E* by $\Delta H =$

$\Delta E + pV$, where T is temperature, p is pressure, and V is volume of system.

$\Delta G^{\ddagger}$ correction. During the DFT calculations, the aqueous molar standard state was considered for all reactions. Due to the change in standard state from 1 atm to 1 M aqueous standard state, the calculated $\Delta G^{\ddagger}$ was corrected by adding 7.9 kJ·mol^{-1} for the reaction type of A → B + C, and reducing 7.9 kJ·mol^{-1} for the reaction type of A + B → C.[4,5]

Descriptor calculation in QSAR modeling. The molecular descriptors of sub-structures of PAE molecules were calculated by Gaussian 09 software[6] and Dragon software (6).[7] With DEP as an example, its molecular structure is:

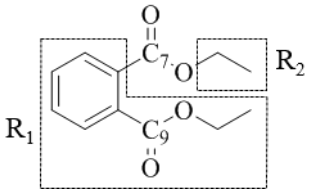

If considering the C_7 side chain of DEP, the descriptors for R_1 was calculated based on the optimized structure as follows:

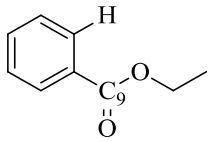

The descriptors for the leaving-group was calculated based on the optimized structure as follows:

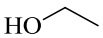

Chemical hardness (η) of molecules was defined by ionization potential (IP) and electron affinity (EA), $\eta = (IP - EA)/2$.[8]

List of molecular descriptors. The quantum chemical descriptors[6] include: partial atomic charges, energy of the highest occupied molecular orbital, energy of the lowest unoccupied molecular orbital, chemical hardness, chemical softness, electronegativity, electrophilic index, polarizability, electron affinity, bond order, and dipole moment.

The Dragon molecular descriptors[7] include: constitutional descriptors, ring descriptors, topological indices, walk and path counts, connectivity indices, information indices, 2D matrix-based descriptors, 2D autocorrelations, burden eigenvalues, edge adjacency indices, geometrical descriptors, 3D matrix-based descriptors, 3D autocorrelations, radial distribution function descriptors, weighted holistic invariant molecular descriptors,

geometric topological and atomic weighted assembly descriptors, randic molecular profiles, functional group counts, atom-centred fragments, atom-type e-state indices, 2D atom pairs, 3D atom pairs, charge descriptors, molecular properties, and drug-like indices.

Standardization of predictor variables. In QSAR modeling, all values of molecular descriptors were standardized by the following formula (1), so as to eliminate the influence of unit and data range of different descriptors.

$$x^* = \frac{x - min}{max - min} \tag{1}$$

where x is the original value, x^* is standardized value, *max* is the maximum value of values corresponding to the descriptor, *min* is the minimum value of values corresponding to the descriptor.

Evaluation of discriminant model. The performance of discriminant model was evaluated by the equations (2) – (6).[9]

$$Accuracy = \frac{TP + TN}{TP + TN + FP + FN} \tag{2}$$

$$Sensitivity = \frac{TP}{TP + FN} \tag{3}$$

$$Specificity = \frac{TN}{TN + FP} \tag{4}$$

$$MCC = \frac{TP \times TN - FP \times FN}{\sqrt{(TP + FP)(TP + FN)(TN + FP)(TN + FN)}} \tag{5}$$

$$Balanced \cdot Accuracy = \frac{TP(TN + FP) + TN(TP + FN)}{2(TP + FN)(TN + FP)} \tag{6}$$

where *TP* represents true positive; *TN* represents true negative; *FP* represents false positive; *FN* represents false negative. In this study, PAEs with departure of leaving-groups as rate-determining steps were classified as positive class, and PAEs with nucleophilic attack of OH^- on the ester bonds as rate-determining steps were classified as negative class.

Characterization of applicability domain of QSAR models. The applicability domain of the QSAR models involved in the present study were characterized by the Williams plot.[10] The standardized residuals (δ), leverage (h) values and warning leverage (h^*)

values were calculated as follows:

$$\delta = \frac{y_i - \hat{y}_i}{\sqrt{\sum_{i=1}^{n}(y_i - \hat{y}_i)^2 / (n - p - 1)}} \quad (7)$$

$$h = x_i^{\mathrm{T}}(X^{\mathrm{T}}X)^{-1}x_i \quad (8)$$

$$h^* = 3(p + 1)/n_{\mathrm{tra}} \quad (9)$$

where y_i and $\hat{y}_i$ are the experimental/DFT calculated values and QSAR predicted values for the *i*-th compound, respectively; n is the number of compounds; p is the number of descriptors; x_i is the descriptor vector of the compound; X is the descriptor matrix; n_{tra} is the number of compounds in the training sets.

Table S1. Experimental k_B values of PAEs and E_a values of carboxylic acid esters

Name	E_a **(kcal·mol^{-1})**	k_B **(mol^{-1}·L·s^{-1})**
DMP	-	$(6.9 \pm 0.3) \times 10^{-2}$
DEP	-	$(2.5 \pm 0.2) \times 10^{-2}$
DBP	-	$(1.0 \pm 0.05) \times 10^{-2}$
DIBP	-	$(1.4 \pm 0.2) \times 10^{-3}$
DEHP		5.09×10^{1}
formic acid methyl ester	9.81	-
acetic acid methyl ester	12.20	-
acetic acid ethyl ester	12.00	-
acetic acid butyl ester	14.30	-
acetic acid propyl ester	12.20	-

Table S2. Comparison of logk_B (mol^{-1}·L·s^{-1}) calculated by B3LYP and M062X functioanls and experimental logk_B for DMP, DEP, DBP, and DIBP, respectively.

		$\Delta G^{\ddagger}$ **(kJ·mol^{-1})**	$v_i^{\ddagger}$	**log$k_{B\text{-DFT}}$**	**log$k_{B\text{-exp}}$**
DMP	B3LYP	57.10	-169.17	3.10	-1.16

		$\Delta G^{\ddagger}$ (kJ·mol^{-1})	$v_i^{\ddagger}$	log$k_{B\text{-}DFT}$	log$k_{B\text{-}exp}$
DEP	M062X	28.78	-231.68	8.15	-1.60
	B3LYP	79.39	-206.79	-0.80	
	M062X	53.01	-281.43	3.98	
DBP	B3LYP	77.27	-201.45	-0.43	-2.00
	M062X	55.35	-274.26	3.58	
DIBP	B3LYP	94.22	-202.61	-3.40	-2.85
	M062X	57.16	-251.36	3.26	
DEHP	B3LYP	64.68	-187.33	1.77	1.71
	M062X	30.13	-180.05	7.82	

Table S3. Comparison between log$k_{B\text{-}DFT}$ calculated with different types of IEFPCM and experimental log$k_{B\text{-}exp}$ for DEP

	$\Delta G^{\ddagger}$ (kJ·mol^{-1})	logk_B (mol^{-1}·L·s^{-1})
B3LYP/6-311++G(2d,2p)/UFF	84.65	-0.80
B3LYP/6-311++G(2d,2p)/Pauling	111.39	-6.42
B3LYP/6-311++G(2d,2p)/Bondi	101.75	-4.74
Experimental value	-	-1.60

Table S4. Effects of explicit water molecules on the base-catalyzed hydrolysis of DEP

	None	1 H_2O	2 H_2O	3 H_2O	Experimental value
$\Delta G^{\ddagger}_{TS1}$ (kJ·mol^{-1})	64.71	73.34	59.67	58.94	-
$\Delta G^{\ddagger}_{TS2}$ (kJ·mol^{-1})	79.39	74.42	62.42	52.05	-
logk_B (mol^{-1}·L·s^{-1})	-0.80	0.06	2.16	2.47	-1.60

Table S5. Errors in the calculated $\Delta G^{\ddagger}$

	DMP	DBP	DIBP	DEHP	DEP	DEP ($1H_2O$)	DEP ($2H_2O$)	DEP ($3H_2O$)
Error ($kJ \cdot mol^{-1}$)	22.50	7.13	-4.52	-4.69	2.61	7.58	19.58	23.06

Table S6. $\Delta G^{\ddagger}$ values of TS_1 and TS_2 for 25 PAEs calculated at the IEFPCM/B3LYP/6-311++G(2d,2p) level

Name	$\Delta G^{\ddagger}_{TS1}$ ($kJ \cdot mol^{-1}$)	$\Delta G^{\ddagger}_{TS2}$ ($kJ \cdot mol^{-1}$)
DMP	57.10	43.03
DEP	64.71	79.39
DPP	64.38	85.02
DAP	68.90	80.36
DBP	64.61	77.27
DIBP	73.39	94.23
DNPP	66.26	81.58
BMPP	66.25	79.89
DNHP	64.52	79.19
DIHP	65.21	81.96
DEHP	64.68	47.79
DIOP	64.53	83.25
DNOP	57.93	77.00
DINP	65.41	73.36
DIDP	63.01	80.50
DUP	65.63	70.02
DIUP	68.11	77.53

Name	$\Delta G^{\ddagger}_{TS1}$ (kJ·mol^{-1})	$\Delta G^{\ddagger}_{TS2}$ (kJ·mol^{-1})
DTDP	50.92	45.04
DCP	74.18	83.52
OBOP_C$_7$	68.24	81.81
OBOP_C$_9$	80.82	93.28
BDP_C$_7$	63.10	78.24
BDP_C$_9$	70.26	67.37
ODP_C$_7$	71.13	71.37
ODP_C$_9$	63.97	72.70
BCP_C$_7$	65.47	82.33
BCP_C$_8$	75.92	80.34
BBP_C$_7$	70.22	61.69
BBP_C$_9$	55.66	68.69
DPHP	73.27	91.14

Table S7. Half-lives ($t_{1/2}$) of PAEs

PAEs	$t_{1/2}$ (hours)		
	pH 7	pH 9	pH 11
DCP	6.52×10^4	6.52×10^2	6.52×10^0
BCP	2.50×10^4	2.50×10^2	2.50×10^0
DEP	1.23×10^4	1.23×10^2	1.23×10^0
DIBP	4.89×10^6	4.89×10^4	4.89×10^2
DBP	5.22×10^3	5.22×10^1	5.22×10^{-1}
DNHP	1.14×10^4	1.14×10^2	1.14×10^0

PAEs	$t_{1/2}$ (hours)		
	pH 7	pH 9	pH 11
BBP	2.15×10^{2}	2.15×10^{0}	2.15×10^{-2}
DIDP	1.92×10^{4}	1.92×10^{2}	1.92×10^{0}
BDP	5.96×10^{2}	5.96×10^{0}	5.96×10^{-2}
DEHP	3.27×10^{1}	3.27×10^{-1}	3.27×10^{-3}
DNOP	4.69×10^{3}	4.69×10^{1}	4.69×10^{-1}
DTDP	1.30×10^{-1}	1.30×10^{-3}	1.30×10^{-5}
ODP	6.15×10^{2}	6.15×10^{0}	6.15×10^{-2}
DMP	1.54×10^{0}	1.54×10^{-2}	1.54×10^{-4}
DPP	1.20×10^{5}	1.20×10^{3}	1.20×10^{1}
DAP	1.83×10^{4}	1.83×10^{2}	1.83×10^{0}
DNPP	2.97×10^{4}	2.97×10^{2}	2.97×10^{0}
DIOP	5.83×10^{4}	5.83×10^{2}	5.83×10^{0}
DUP	2.80×10^{2}	2.80×10^{0}	2.80×10^{-2}
OBOP	6.59×10^{4}	6.59×10^{2}	6.59×10^{0}
DINP	1.08×10^{3}	1.08×10^{1}	1.08×10^{-1}
DIUP	5.80×10^{3}	5.80×10^{1}	5.80×10^{-1}
DPHP	1.41×10^{6}	1.41×10^{4}	1.41×10^{2}
DIHP	3.48×10^{4}	3.48×10^{2}	3.48×10^{0}
BMPP	1.53×10^{4}	1.53×10^{2}	1.53×10^{0}

Table S8. Influence of alkyl side chain type on hydrolysis kinetics of PAEs

Number of C atoms in R groups	PAEs	$k_{B\text{-}DFT}$ or $k_{B\_side\ chain}$ ($mol^{-1}\cdot L\cdot s^{-1}$)
4 C atoms	DIBP	3.94×10^{-4}
	DBP	3.69×10^{-1}
6 C atoms	BMPP	1.26×10^{-1}
	DNHP	1.69×10^{-1}
8 C atoms	DIOP	3.30×10^{-2}
	DNOP	4.10×10^{-1}
10 C atoms	DPHP	6.84×10^{-4} ($\log k_{B\_side\ chain}$)
	BDP_C_9 side chain	3.11×10^{0} ($\log k_{B\_C9}$)
	ODP_C_9 side chain	1.16×10^{0} ($\log k_{B\_C9}$)
13 C atoms	DIUP	3.32×10^{-1}
	DTDP	1.50×10^{4}

Table S9. Values of molecular descriptors in models

PAEs	D_1	D_2	D_3	D_4	D_5	D_6	D_7
DINP	-0.105	-0.269	0.989	0.0977	2.00	9.00	-
BDP_C_9	-0.127	-0.271	0.990	-	-	-	322
DBP	-0.108	-0.272	0.989	0.0990	0.00	4.00	-
DEP	-0.110	-0.272	0.990	0.0992	0.00	2.00	-
BDP_C_7	-0.104	-0.269	0.990	0.0979	0.00	4.00	-
BBP_C_7	-0.123	-0.265	0.992	-	-	-	322
BCP_C_7	-0.108	-0.271	0.990	0.0990	0.00	4.00	-
DCP	-0.112	-0.271	0.990	0.0993	0.00	6.00	-

PAEs	D_1	D_2	D_3	D_4	D_5	D_6	D_7
DIHP	-0.107	-0.270	0.990	0.0980	2.00	7.00	-
DPHP	-0.104	-0.269	0.990	0.101	2.00	10.0	-
ODP_C$_7$	-0.127	-0.272	0.989	0.0977	0.00	8.00	-
DIBP	-0.113	-0.272	0.990	0.0993	2.00	4.00	-
DUP	-0.123	-0.271	0.990	0.0978	0.00	11.0	-
DIOP	-0.104	-0.270	0.990	0.0979	2.00	8.00	-
DNPP	-0.101	-0.270	0.989	0.0977	0.00	5.00	-
DAP	-0.108	-0.272	0.990	0.0975	0.00	1.00	-
BCP_C$_8$	-0.118	-0.272	0.990	0.0990	0.00	6.00	-
DMP	-0.129	-0.271	0.988	-	-	-	176
DTDP	-0.124	-0.270	0.988	-	-	-	567
DNOP	-0.105	-0.272	0.990	0.0980	0.00	8.00	-
DIDP	-0.101	-0.269	0.990	0.0981	2.00	10.0	-
DNHP	-0.100	-0.270	0.988	0.0982	0.00	6.00	-
BBP_C$_9$	-0.110	-0.270	0.992	0.0945	0.00	1.00	-
ODP_C$_9$	-0.106	-0.270	0.989	0.0977	0.00	10.0	-
BMPP	-0.101	-0.269	0.987	0.0977	2.00	6.00	-
DIUP	-0.106	-0.270	0.990	0.0978	2.00	13.0	-
DPP	-0.106	-0.272	0.990	0.0992	0.00	3.00	-
DEHP	-0.122	-0.269	0.987	-	-	-	405

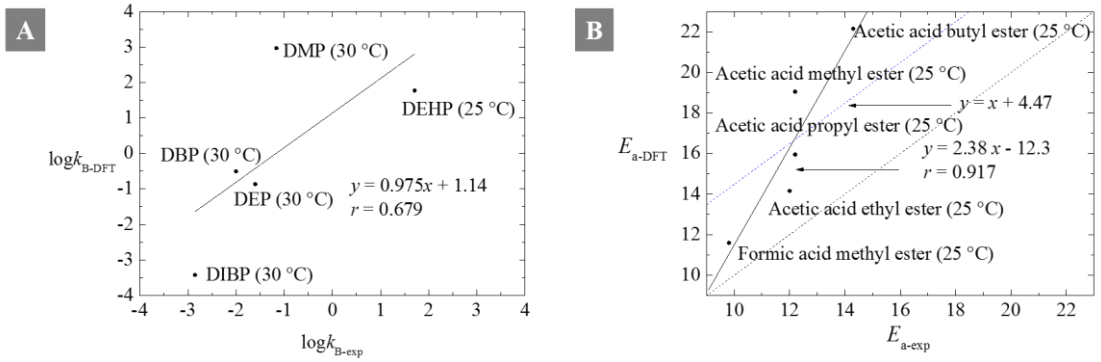

Figure S1. Linear correlation between DFT calculated values at IEFPCM(UFF)/B3LYP/6-311++G(2d,2p) level and corresponding experimental values (The solid lines are fitted by least-squares analysis; the dashed lines are the reference lines with slope = 1).

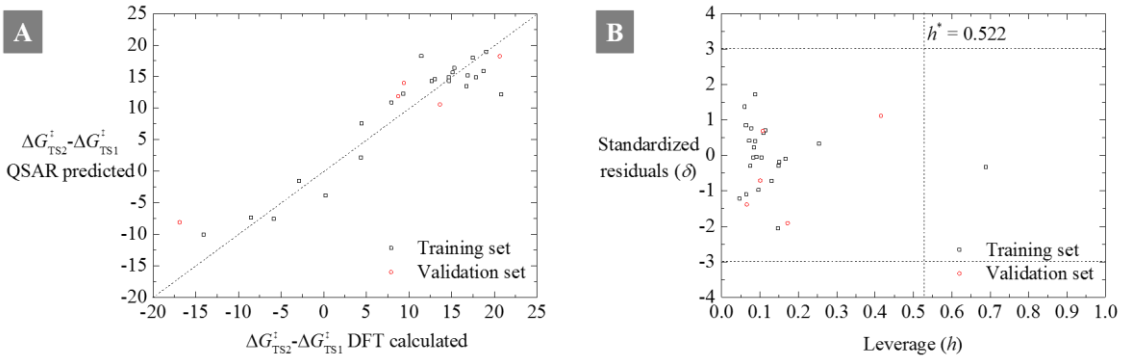

Figure S2. (A) Plot for predicted $\Delta G^{\ddagger}_{TS2}$-$\Delta G^{\ddagger}_{TS1}$ values versus DFT calculated $\Delta G^{\ddagger}_{TS2}$-$\Delta G^{\ddagger}_{TS1}$ values; (B) Williams plot indicating applicability domain of the discriminant model (3).

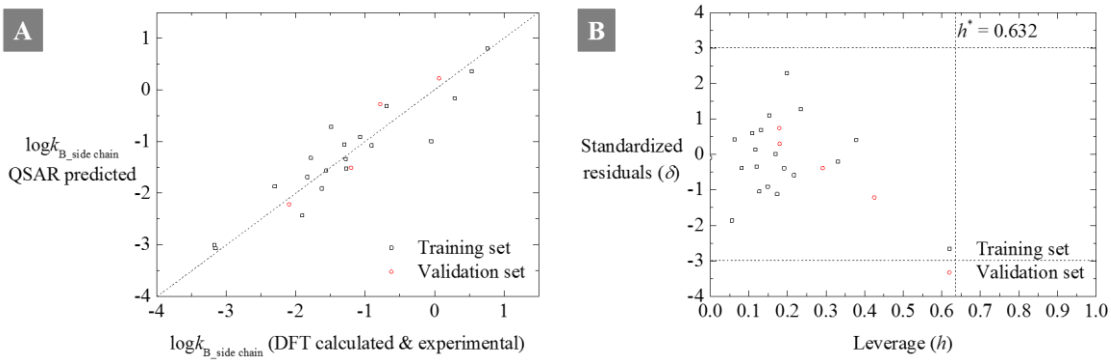

Figure S3. (A) Plot for model (4) predicted $\log k_{B\_side\ chain}$ values versus DFT calculated and experimental $\log k_{B\_side\ chain}$ values; (B) Williams plot indicating applicability domain

of the QSAR model (4).

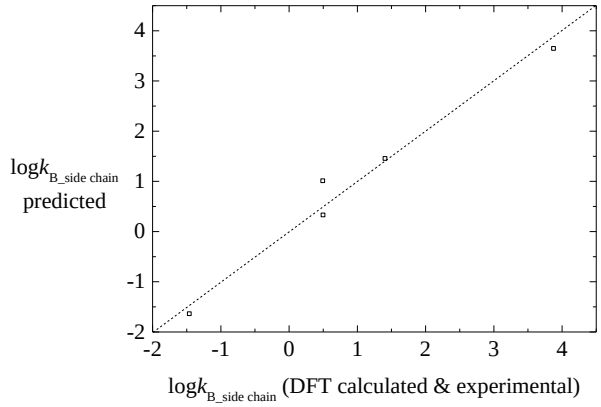

Figure S4. Plot for model (5) predicted log$k_{B_side\ chain}$ values versus DFT calculated and experimental log$k_{B_side\ chain}$ values.

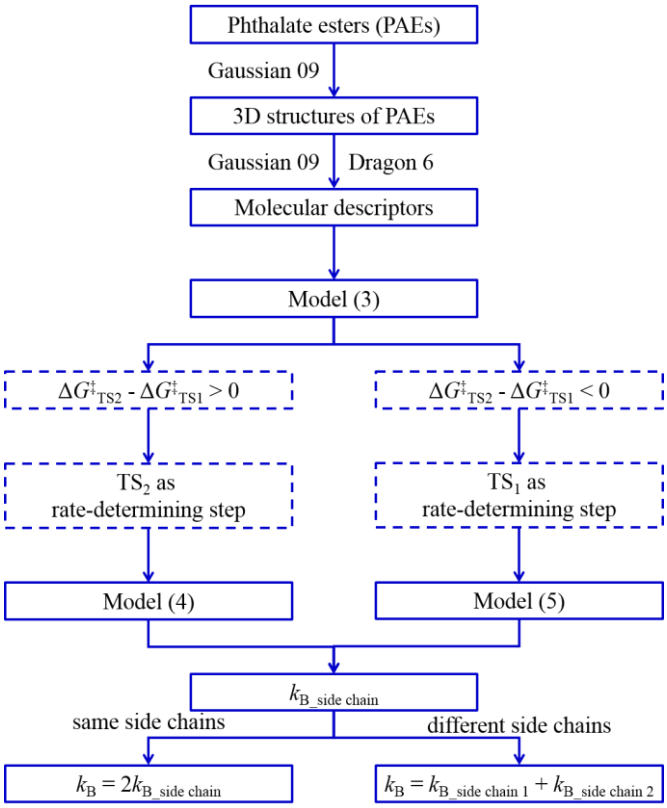

Figure S5. Procedure of predicting k_B values of PAEs (TS_1 represents nucleophilic attack of OH^- on ester bonds, TS_2 represents departure of leaving-groups, $\Delta G^{\ddagger}$ represents Gibbs free energy difference between TS and reactants, $k_{B\_side\ chain}$ represents second-order rate constants for base-catalyzed hydrolysis of one side chain in PAEs, k_B represents second-order rate constant for base-catalyzed hydrolysis).

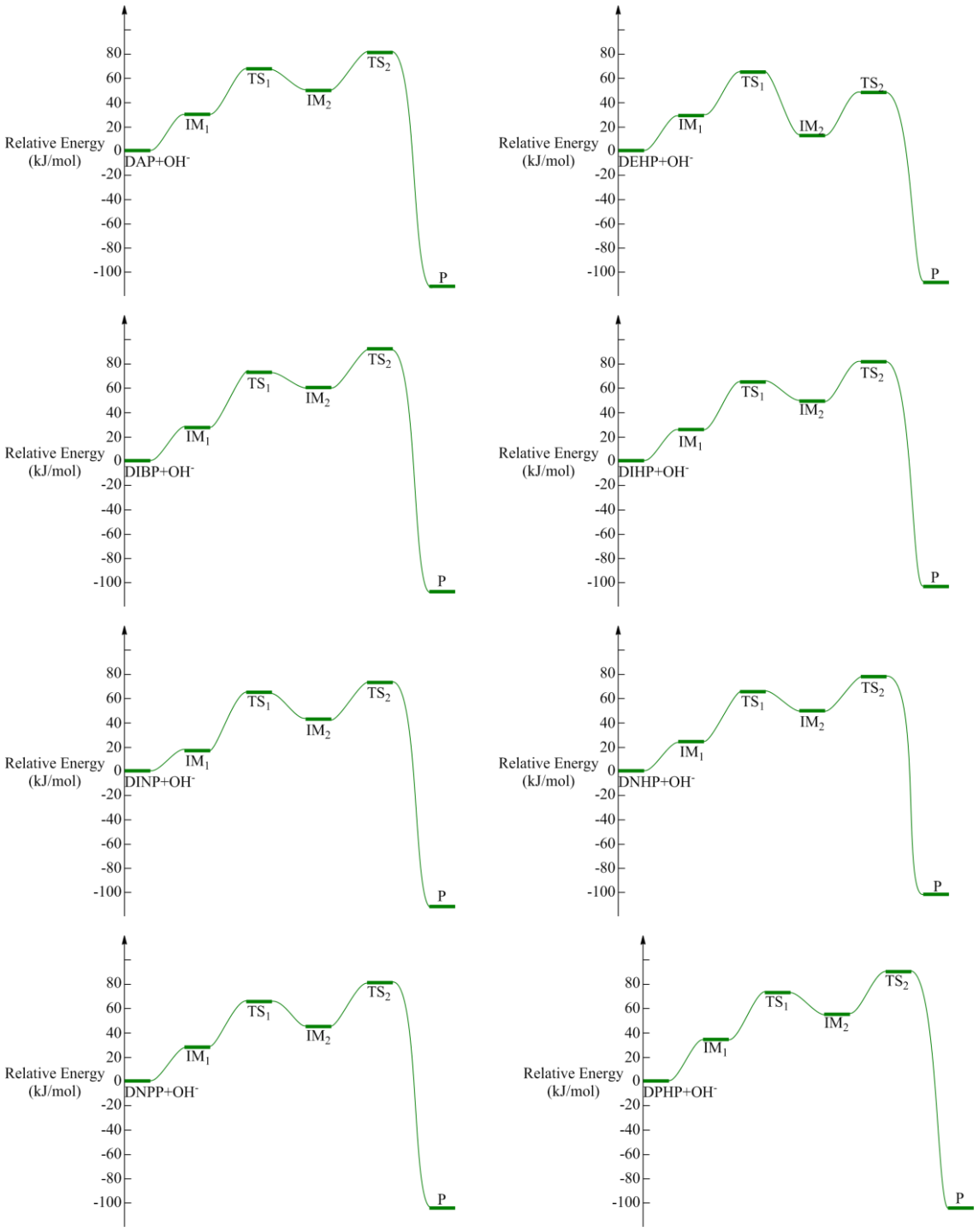

Figure S6. Schematic free energy surfaces for base-catalyzed hydrolysis of the PAEs calculated at IEFPCM/B3LYP/6-311++G(2d,2p) level [The total energy of the reactants and OH^- is set to zero (reference state). The symbols "IM_1, TS, IM_2, P" refer to pre-reactive complexes, transition states, intermediates and products involved in the reaction, respectively]

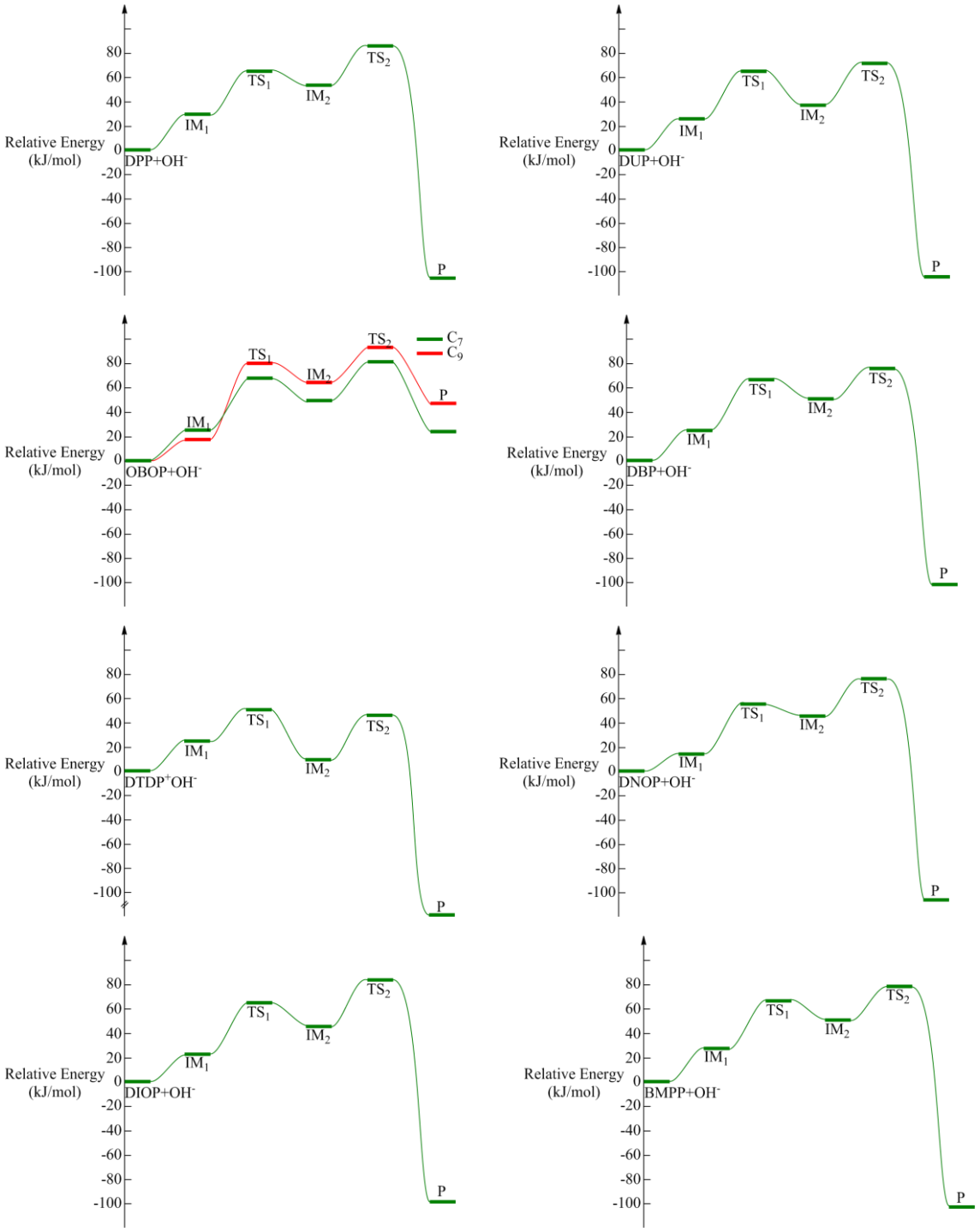

Figure S6. Schematic free energy surfaces for base-catalyzed hydrolysis of the PAEs calculated at IEFPCM/B3LYP/6-311++G(2d,2p) level [The total energy of the reactants and OH^- is set to zero (reference state). The symbols "IM_1, TS, IM_2, P" refer to pre-reactive complexes, transition states, intermediates and products involved in the reaction, respectively]

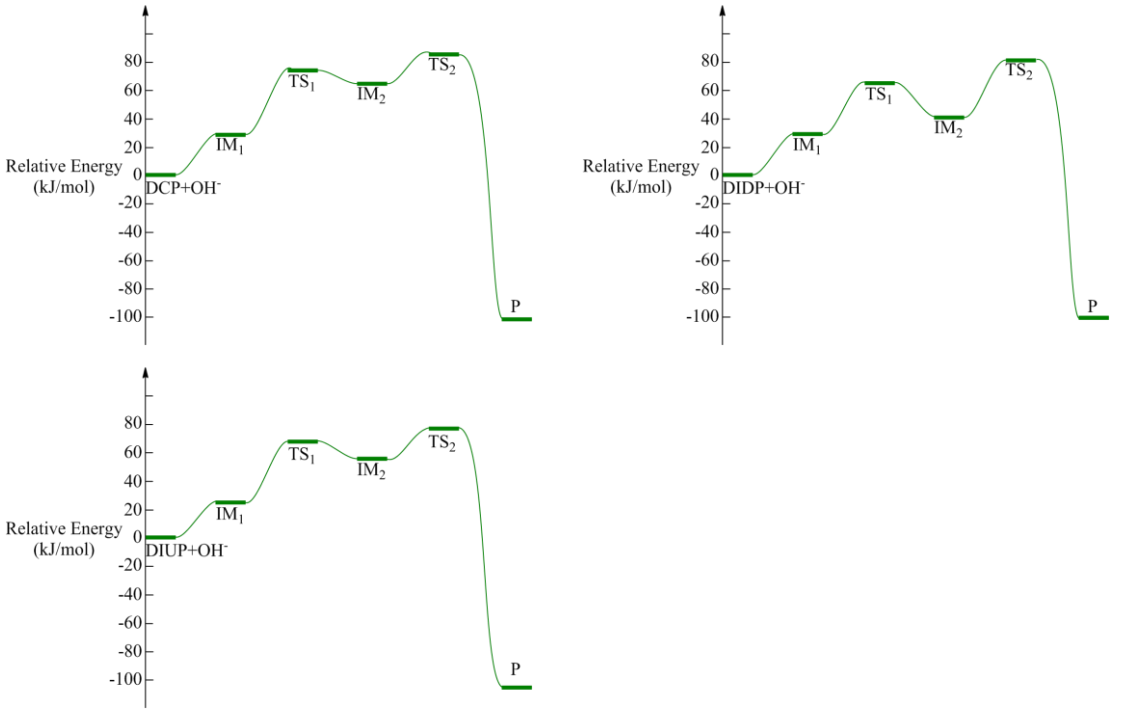

Figure S6. Schematic free energy surfaces for base-catalyzed hydrolysis of the PAEs calculated at IEFPCM/B3LYP/6-311++G(2d,2p) level [The total energy of the reactants and OH^- is set to zero (reference state). The symbols "IM_1, TS, IM_2, P" refer to pre-reactive complexes, transition states, intermediates and products involved in the reaction, respectively]

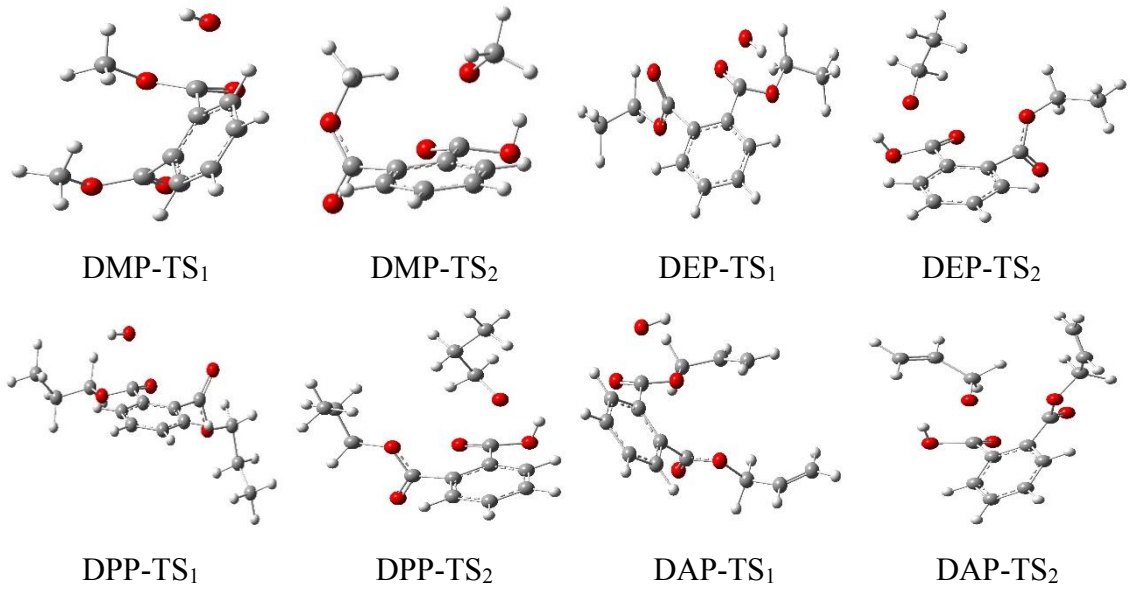

Figure S7. Structures of transition states (TS) of PAEs

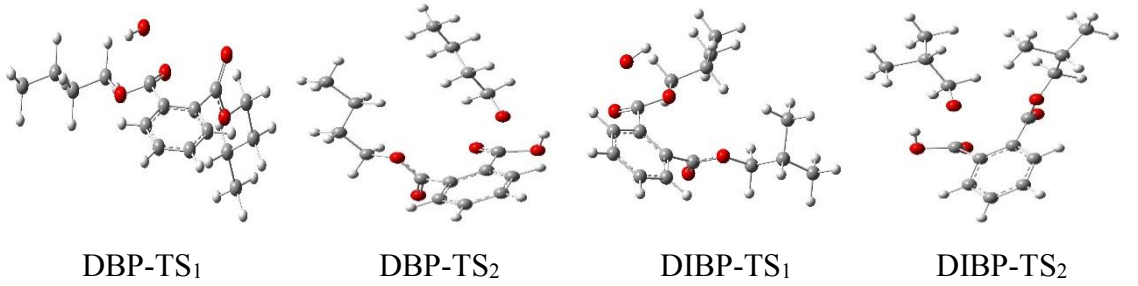

DBP-TS$_1$ DBP-TS$_2$ DIBP-TS$_1$ DIBP-TS$_2$

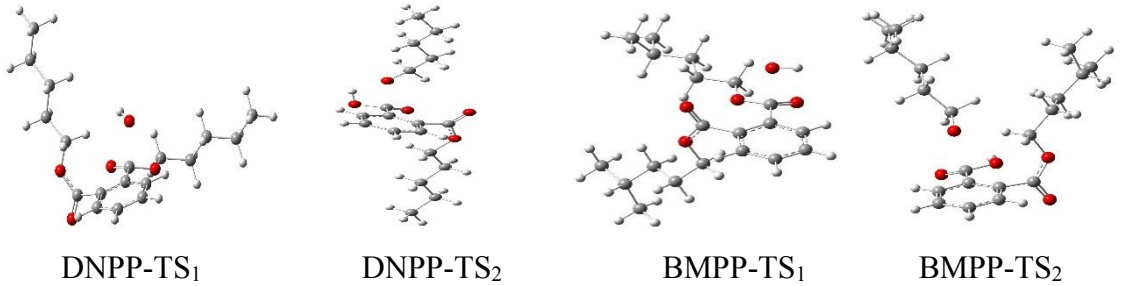

DNPP-TS$_1$ DNPP-TS$_2$ BMPP-TS$_1$ BMPP-TS$_2$

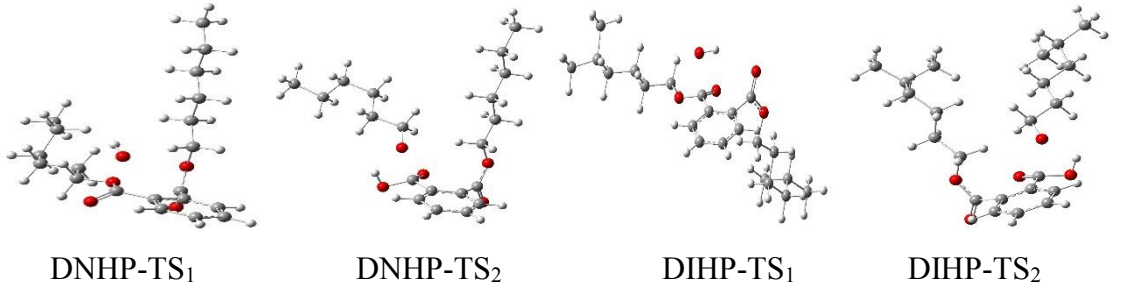

DNHP-TS$_1$ DNHP-TS$_2$ DIHP-TS$_1$ DIHP-TS$_2$

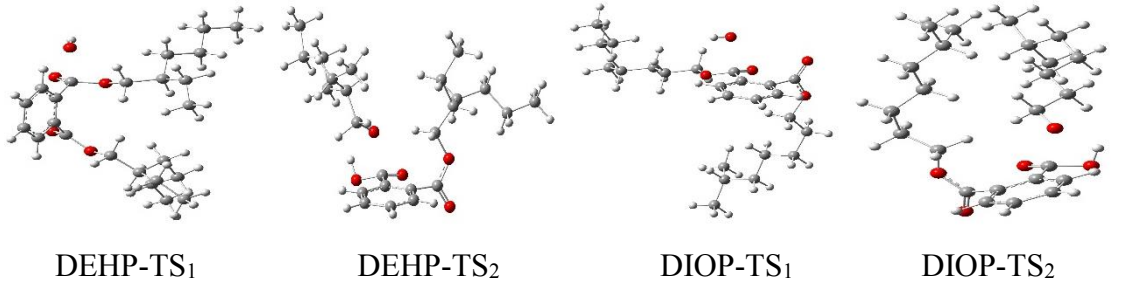

DEHP-TS$_1$ DEHP-TS$_2$ DIOP-TS$_1$ DIOP-TS$_2$

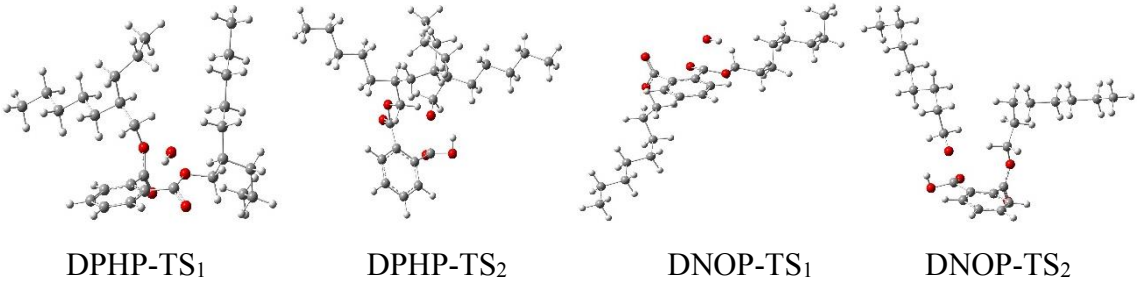

DPHP-TS$_1$ DPHP-TS$_2$ DNOP-TS$_1$ DNOP-TS$_2$

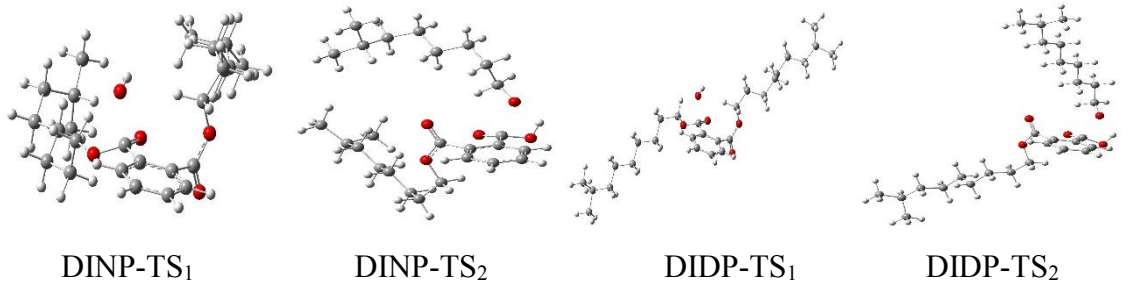

DINP-TS$_1$ DINP-TS$_2$ DIDP-TS$_1$ DIDP-TS$_2$

Figure S7. Structures of transition states (TS) of PAEs

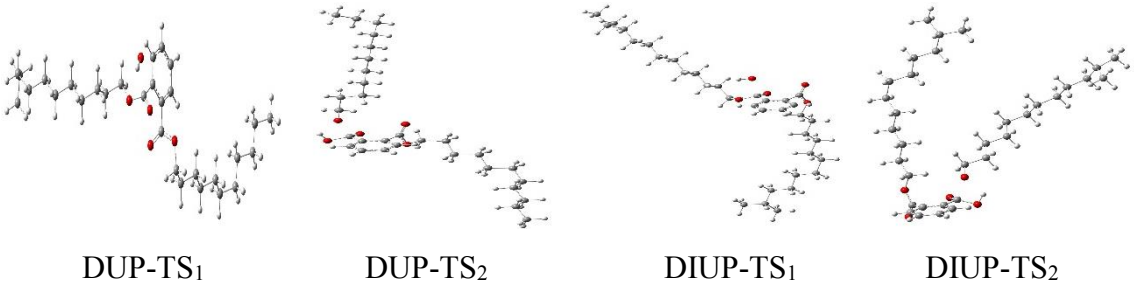

DUP-TS_1 DUP-TS_2 DIUP-TS_1 DIUP-TS_2

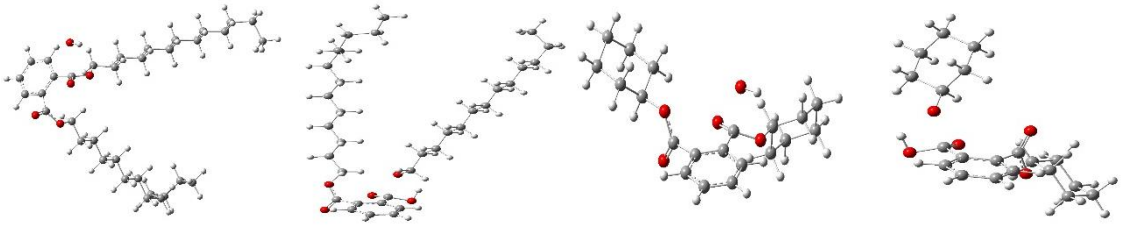

DTDP-TS_1 DTDP-TS_2 DCP-TS_1 DCP-TS_2

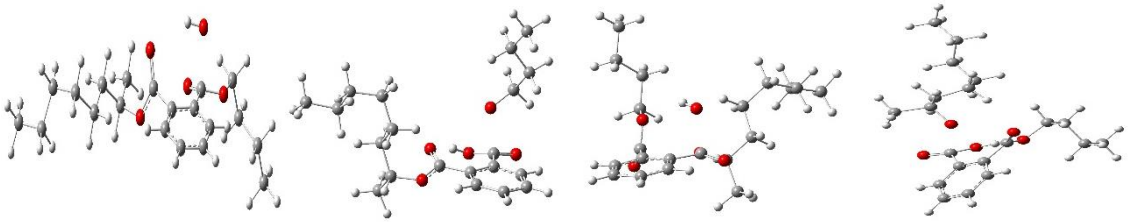

OBOP-C_7-TS_1 OBOP-C_7-TS_2 OBOP-C_9-TS_1 OBOP-C_9-TS_2

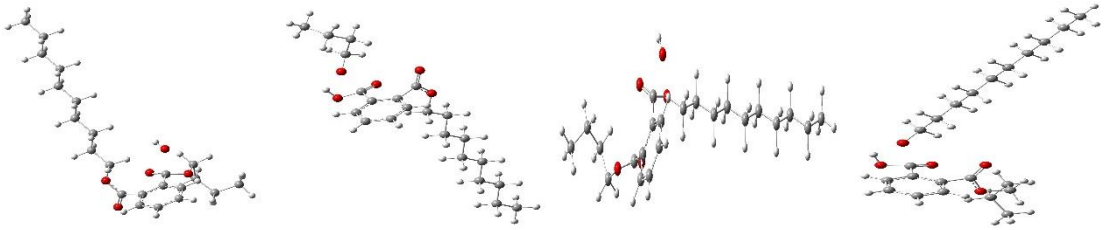

BDP-C_7-TS_1 BDP-C_7-TS_2 BDP-C_9-TS_1 BDP-C_9-TS_2

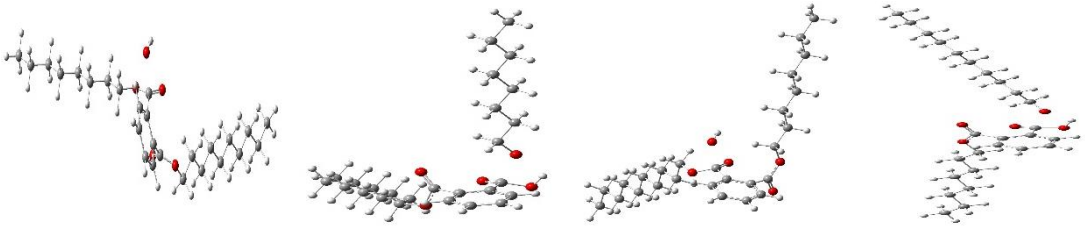

ODP-C_7-TS_1 ODP-C_7-TS_2 ODP-C_9-TS_1 ODP-C_9-TS_2

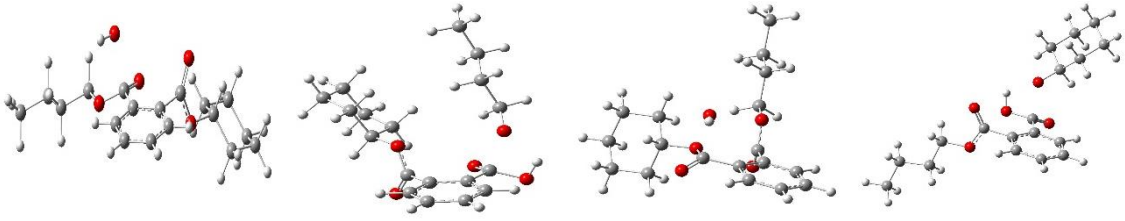

BCP-C_7-TS_1 BCP-C_7-TS_2 BCP-C_8-TS_1 BCP-C_8-TS_2

Figure S7. Structures of transition states (TS) of PAEs

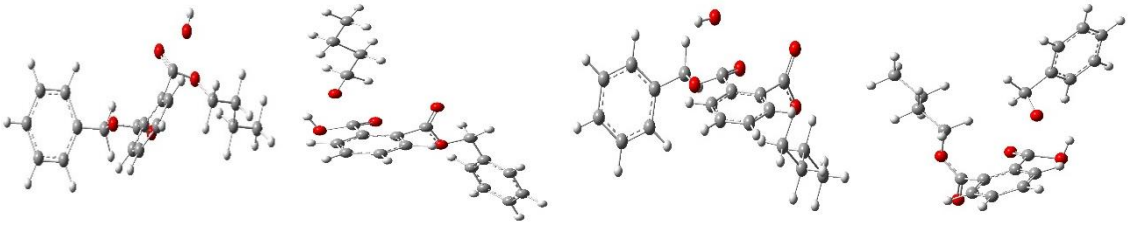

BBP-C_7-TS_1 BBP-C_7-TS_2 BBP-C_9-TS_1 BBP-C_9-TS_2

Figure S7. Structures of transition states (TS) of PAEs

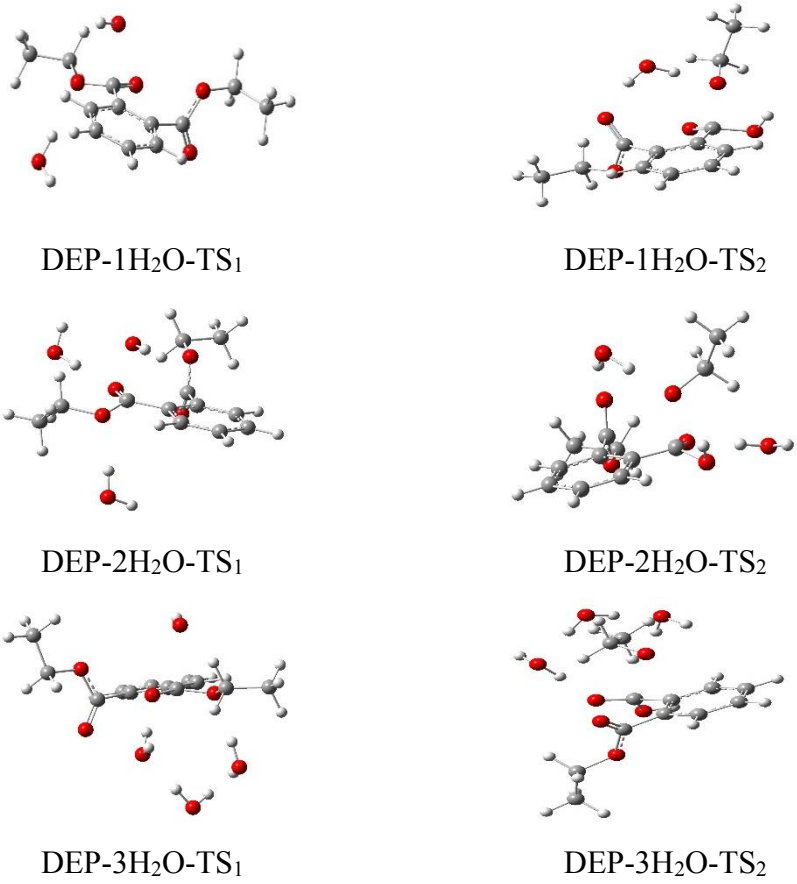

DEP-1H_2O-TS_1 DEP-1H_2O-TS_2

DEP-2H_2O-TS_1 DEP-2H_2O-TS_2

DEP-3H_2O-TS_1 DEP-3H_2O-TS_2

Figure S8. Structures of transition states (TS) of DEP with 1 - 3 explicit water molecules

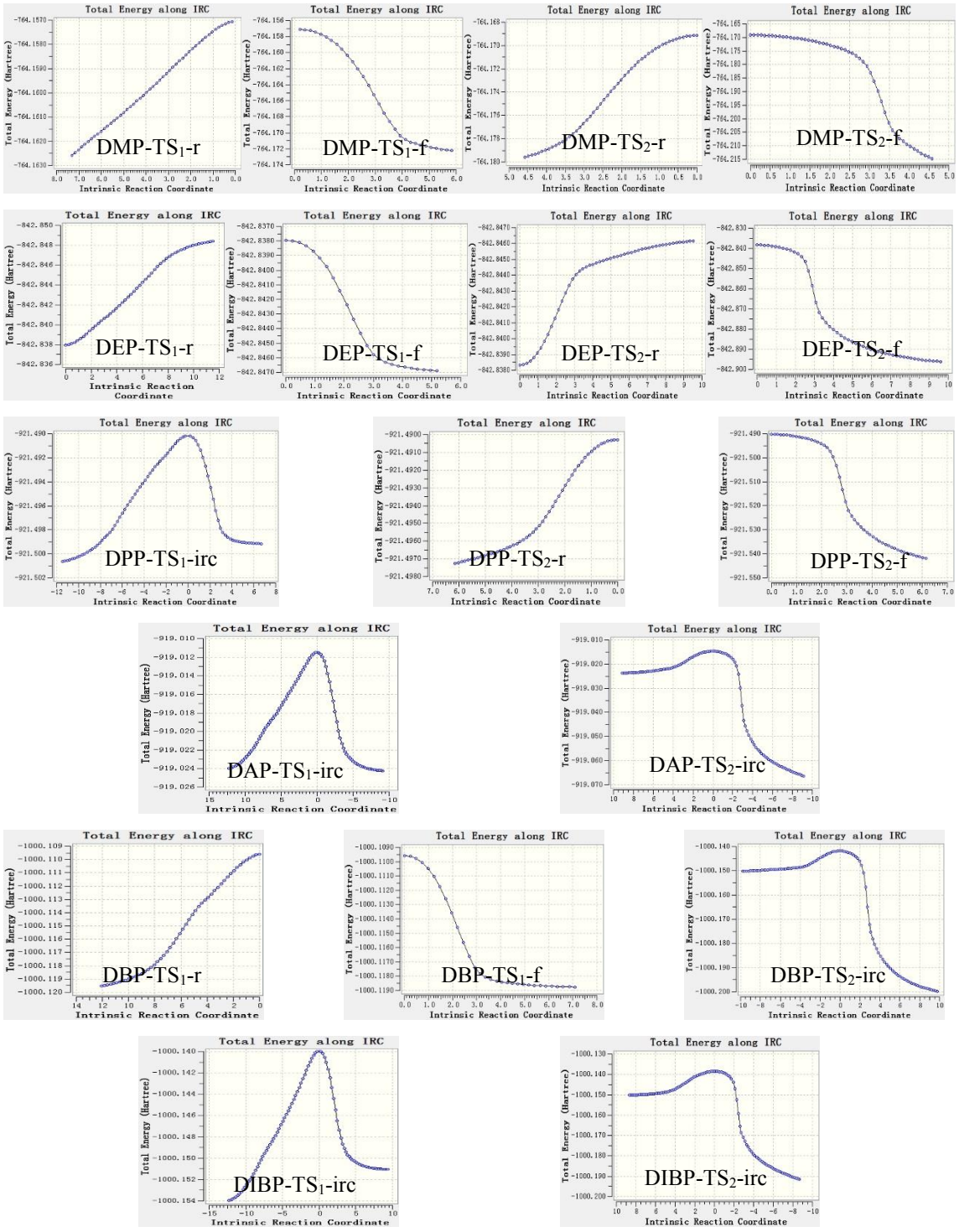

Figure S9. Intrinsic reaction coordinate (IRC) calculation results of the transition states (TS) of PAEs calculated at IEFPCM/B3LYP/6-311++G(2d,2p) level (The symbols "r and f" refer to reverse and forward, respectively.)

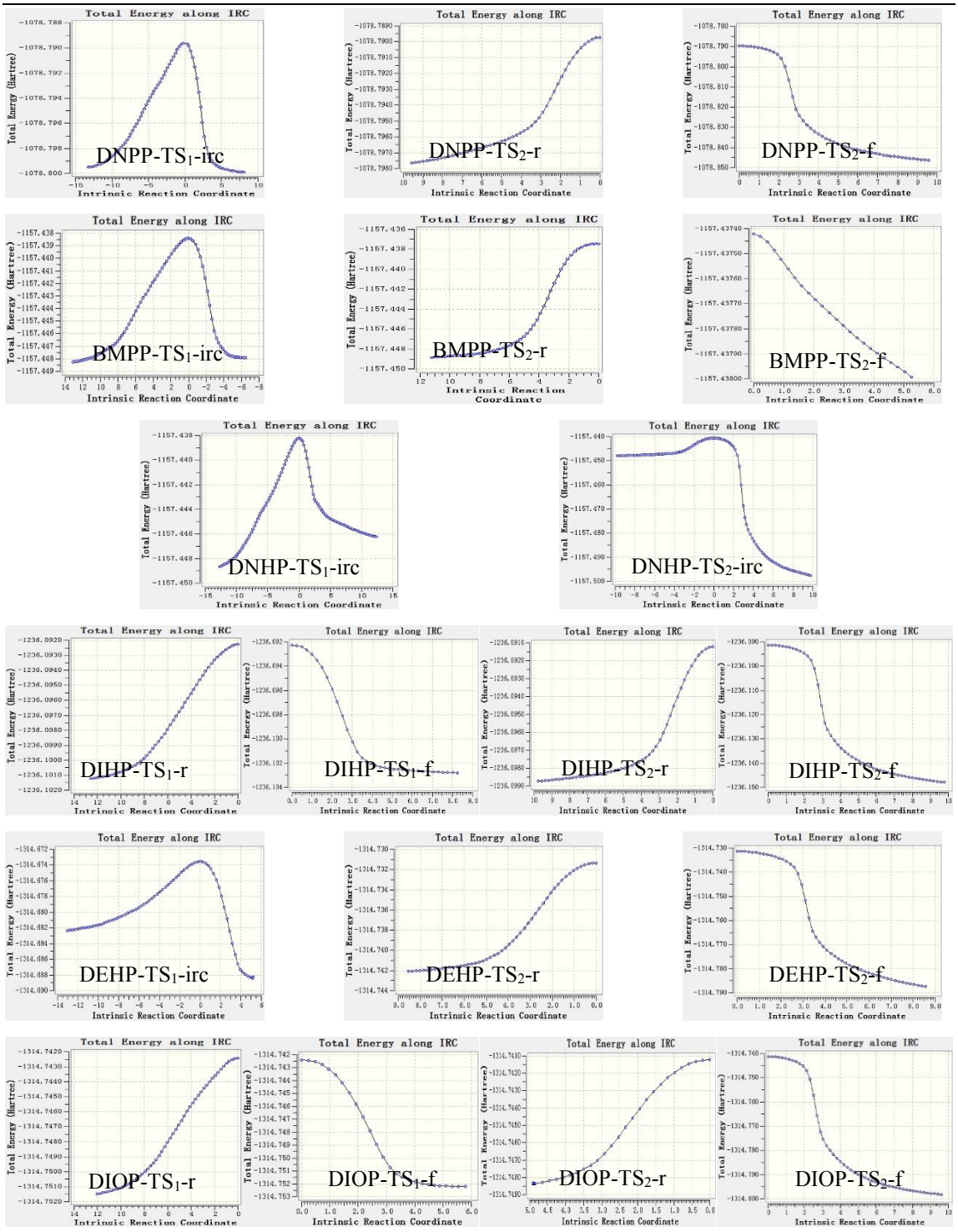

Figure S9. Intrinsic reaction coordinate (IRC) calculation results of the transition states (TS) of PAEs calculated at IEFPCM/B3LYP/6-311++G(2d,2p) level (The symbols "r and f" refer to reverse and forward, respectively.)

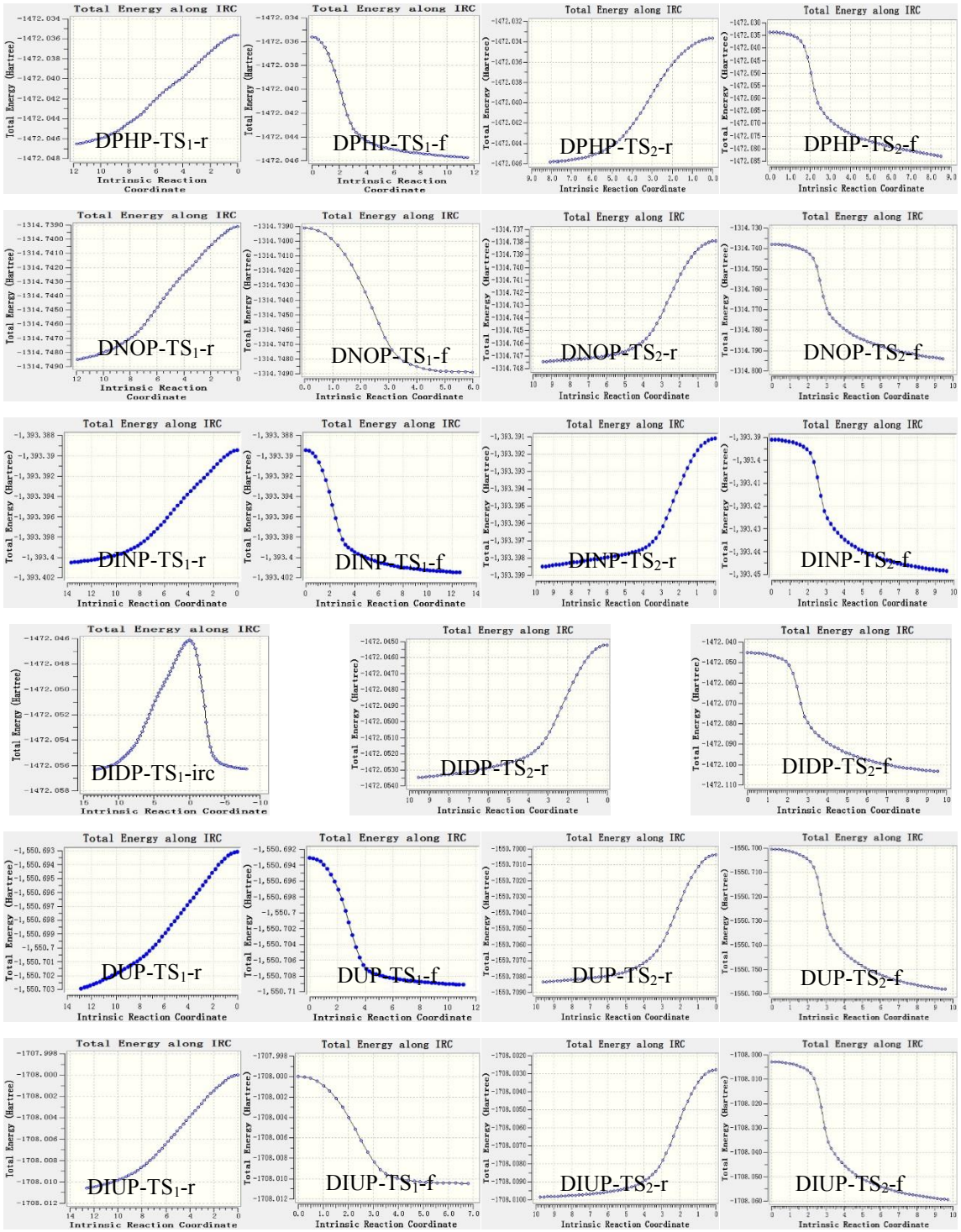

Figure S9. Intrinsic reaction coordinate (IRC) calculation results of the transition states (TS) of PAEs calculated at IEFPCM/B3LYP/6-311++G(2d,2p) level (The symbols "r and f" refer to reverse and forward, respectively.)

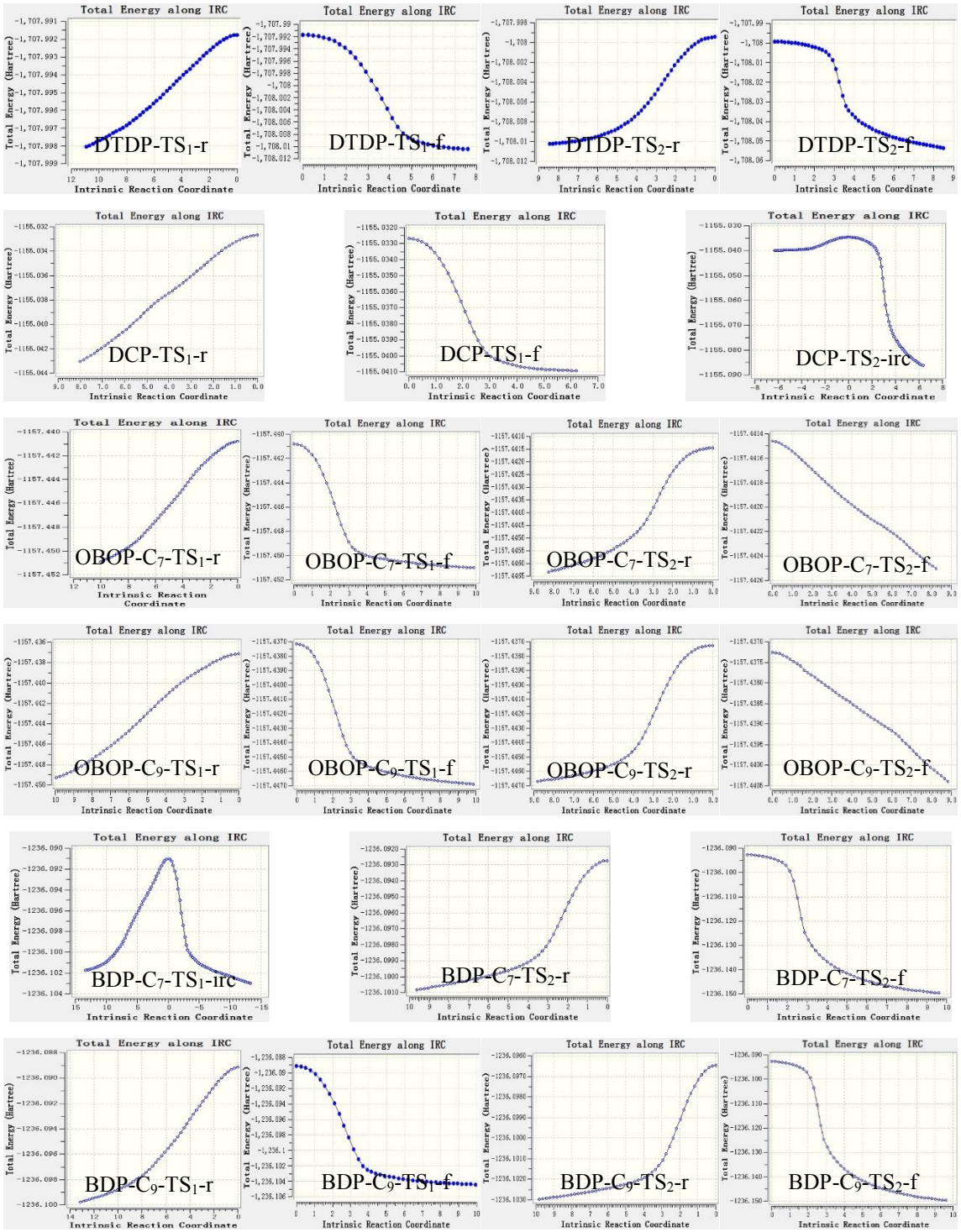

Figure S9. Intrinsic reaction coordinate (IRC) calculation results of the transition states (TS) of PAEs calculated at IEFPCM/B3LYP/6-311++G(2d,2p) level (The symbols "r and f" refer to reverse and forward, respectively.)

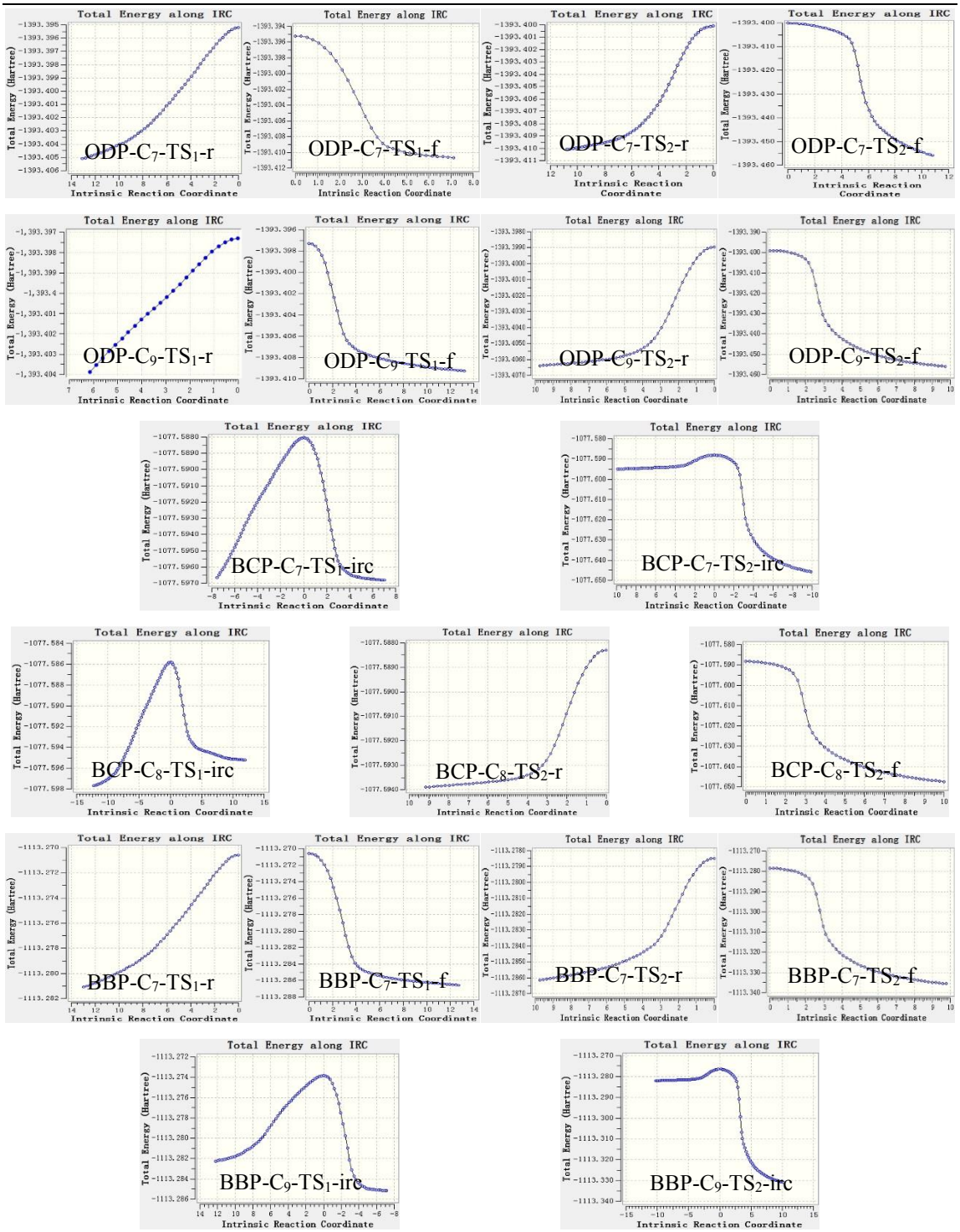

Figure S9. Intrinsic reaction coordinate (IRC) calculation results of the transition states (TS) of PAEs calculated at IEFPCM/B3LYP/6-311++G(2d,2p) level (The symbols "r and f" refer to reverse and forward, respectively.)

References

(1) Ahlrichs, R.; Bär, M.; Häser, M.; Horn, H.; Kölmel, C. Electronic – structure calculations on workstation computers – The program system turbomole. *Chem.*

Phys. Lett. 1989, *162* (3), 165-169.

(2) Gill, P. M. W.; Johnson, B. G.; Pople, J. A. The performance of the Becke-Lee-Yang-Parr (B-LYP) density functional theory with various basis sets. *Chem. Phys. Lett.* 1992, *197* (4-5), 499-505.

(3) Li, C.; Xie, H. B.; Chen, J. W.; Yang, X. H.; Zhang, Y. F.; Qiao, X. L. Predicting gaseous reaction rates of short chain chlorinated paraffins with ·OH: Overcoming the difficulty in experimental determination. *Environ. Sci. Technol*. 2014, *48* (23), 13808-13816.

(4) Sviatenko, L. K.; Gorb, L.; Hill, F. C.; Leszczynska, D.; Shukla, M. K.; Okovytyy, S. I.; Hovorun, D.; Leszczynski, J. In silico alkaline hydrolysis of octahydro – 1,3,5,7 – tetranitro – 1,3,5,7 – tetrazocine: Density Functional Theory investigation. *Environ. Sci. Technol*. 2016, *50* (18), 10039-10046.

(5) Zhang, H. Q.; Xie, H. B.; Chen, J. W.; Zhang, S. S. Prediction of hydrolysis pathways and kinetics for antibiotics under environmental pH conditions: A quantum chemical study on cephradine. *Environ. Sci. Technol*. 2015, *49* (3), 1552-1558.

(6) Frisch, M. J.; Trucks, G. W.; Schlegel, H. B.; Scuseria, G. E.; Robb, M. A.; Cheeseman, J. R.; Scalmani, G.; Barone, V.; Mennucci, B.; Petersson, G. A.; Nakatsuji, H.; Caricato, M.; Li, X.; Hratchian, H. P.; Izmaylov, A. F.; Bloino, J.; Zheng, G.; Sonnenberg, J. L.; Hada, M.; Ehara, M.; Toyota, K.; Fukuda, R.; Hasegawa, J.; Ishida, M.; Nakajima, T.; Honda, Y.; Kitao, O.; Nakai, H.; Vreven, T.; Montgomery, J. A., Jr.; Peralta, J. E.; Ogliaro, F.; Bearpark, M.; Heyd, J. J.; Brothers, E.; Kudin, K. N.; Staroverov, V. N.; Kobayashi, R.; Normand, J.; Raghavachari, K.; Rendell, A.; Burant, J. C.; Iyengar, S. S.; Tomasi, J.; Cossi, M.; Rega, N.; Millam, J. M.; Klene, M.; Knox, J. E.; Cross, J. B.; Bakken, V.; Adamo, C.; Jaramillo, J.; Gomperts, R.; Stratmann, R. E.; Yazyev, O.; Austin, A. J.; Cammi, R.; Pomelli, C.; Ochterski, J. W.; Martin, R. L.; Morokuma, K.; Zakrzewski, V. G.; Voth, G. A.; Salvador, P.; Dannenberg, J. J.; Dapprich, S.; Daniels, A. D.; Farkas, O.; Foresman, J. B.; Ortiz, J. V.; Cioslowski, J.; Fox, D. J. Gaussian 09, Revision A.01; Gaussian, Inc.: Wallingford CT, 2009.

(7) Talete srl, DRAGON (Software for Molecular Descriptor Calculation) Version 6.0, 2012, http://www.talete.mi.it (accessed 2018.03.17).

(8) Chang, C. M.; Lin, T. H.; Chen, Y. S.; Chang, C. W.; Huang, K. L.; Wu, F. W.; Hsu, W. J.; Yu, M. P.; Lin, C.; Wang, M. K. A quantum chemical approach using classical

concepts to characterization and descriptive analysis of various reactions of metal ions and organic compounds. *Chemometr. Intell. Lab*. 2014, *136*, 155-163.

(9) Hong, H.; Thakkar, S.; Chen, M.; Tong, W. Development of decision forest models for prediction of drug-induced liver injury in humans using a large set of FDA-approved drugs. *Sci. Rep*. 2017, *7* (1), 1-15.

(10) Li, X. H.; Zhao, W. X.; Li, J.; Jiang, J. Q.; Chen, J. J.; Chen, J. W. Development of a model for predicting reaction rate constants of organic chemicals with ozone at different temperatures. *Chemosphere* 2013, *92* (8), 1029-1034.